第 32 卷第 1 期 无 机 化 学 学 报 Vol.32 No.1
2016 年 1 月 CHINESE JOURNAL OF INORGANIC CHEMISTRY 121-138

含苯并咪唑基配体钴(Ⅱ)配合物的合成、晶体结构和儿茶酚酶活性

张 前[1] 韩 燕[2] 焦元红*,[1]
([1]湖北理工学院化学与化工学院,黄石 435003)
([2]新乡学院化学化工学院,新乡 453003)

摘要:合成和表征了一种钴(Ⅱ)配合物,$[CoLCl]_2[CoLCl_{0.5}(H_2O)_{0.5}]_2ClO_4\cdot 10H_2O$ (**1**)(LH=(2-(二((1*H*-苯并咪唑-2-基)甲基)氨基)乙酸))。以 3,5-二叔丁基儿茶酚(3,5-DTBC)为反应底物,用紫外光谱测试了 **1** 的儿茶酚酶催化活性。研究结果表明:在配合物的晶体结构中,不对称单元的 2 个 Co(Ⅱ)都形成变形的三角双锥构型。在 pH=5~11 范围内,配合物 **1** 对 3,5-DTBC 的氧化显示了 pH 值依赖性,它的儿茶酚酶催化活性随着温度的升高而升高,并且其催化氧化 3,5-DTBC 的动力学符合米氏方程模型。

关键词:钴(Ⅱ)配合物;晶体结构;儿茶酚酶;催化活性
中图分类号:O614.81+2 **文献标识码**:A **文章编号**:1001-4861(2016)01-0131-08
DOI:10.11862/CJIC.2016.031

Synthesis, Crystal Structure and Catecholase Activity of the Cobalt(Ⅱ) Complex Containing Benzimidazole Ligand

ZHANG Qian[1] HAN Yan[2] JIAO Yuan-Hong*,[1]
([1]*College of Chemistry and Chemical Engineering, Hubei Polytechnic University, Huangshi, Hubei* 435003, *China*)
([2]*College of Chemistry and Chemical Engineering, Xinxiang University, Xinxiang, Henan* 453003, *China*)

Abstract: A cobalt(Ⅱ) complex, $[CoLCl]_2[CoLCl_{0.5}(H_2O)_{0.5}]_2ClO_4\cdot 10H_2O$ (**1**) (LH=(2-(bis((1*H*-benzo[d]-imidazol-2-yl) methyl)amino)acetic acid)) has been synthesized and characterized. Its catecholase catalytic activity has been exploited by UV-Vis spectrophotometric study by using 3,5-di-*tert*-butylcatechol (3,5-DTBC) as the substrate. The results showed that two cobalt(Ⅱ) ions of the asymmetric unit were both coordinated by the ligands in a distorted trigonal-bipyramidal geometry in the crystal structure. Complex **1** exhibited pH value dependence for the oxidation of 3,5-DTBC in the range of pH 5 to 11, and its catecholase catalytic activity increased with increasing temperature. The kinetics of oxidation of 3,5-DTBC catalyzed by complex **1** accorded with the Michaelis-Mentent equation. CCDC: 950329, **1**.

Keywords: cobalt(Ⅱ) complex; crystal structure; catecholase; catalytic activity

Catecholase (EC 1.10.3.1) is a type-3 copper enzyme usually encountered in plant tissues and in some insects and crustaceans. It catalyzes the oxidation of a broad range of *o*-diphenols to the corresponding *o*-quinones coupled with the reduction of oxygen to water[1]. Catecholase is of economic importance due to its help to protect damaged plants against both bacterial and fungal disease. In the crystal structure of catecholase isolated from Ipomoea batatas (sweet potato), the active site contains a binuclear copper(Ⅱ)

收稿日期:2015-07-21。收修改稿日期:2015-11-16。
湖北省教育厅 B 类项目(No.B20114404,B2013067)资助。
*通信联系人。E-mail:yhjiao2014@163.com

center, and each copper(Ⅱ) ion is coordinated by three imidazole nitrogen atoms from three histidine units[2]. It′ s inspired numerous scientists to study the structure-activity relationships of catecholase. Benzimidazole could mimic the histidine residue owing to its same imidazole group, and recently many catecholase model complexes containing benzimidazole and imidazole ligands have been reported based on their active sites[3-8]. The synthesis of artificial catecholase could provide a deeper insight into the structure, catalytic activity and mechanism of the natural catecholase, and it helps us to design more effective catecholase models. Herein, we report the synthesis and crystal structure of a cobalt (Ⅱ) complex (**1**) containing benzimidazole ligand. Furthermore, its catecholase catalytic activity was investigated using 3,5-di-*tert*-butylcatechol (3,5-DTBC) as the substrate.

1 Experimental

1.1 Materials and physical measurements

All reagents were purchased from commercial companies and directly used unless stated otherwise. The melting point was determined with an XT4A micromelting point apparatus and was uncorrected. The pH value was adjusted by PHS-3C digital pH meter. UV-Vis spectra were measured on an Analytik jena Specord 210 spectrophotometer. The IR spectra were carried out on a Perkin-Elmer Spectrum BX FT-IR instrument in tablets with potassium bromide. Elemental analyses were examined on a Perkin-Elmer 2400 instrument. Electrospray ionization mass spectra (ESI-MS) were performed on an Applied Biosystems API 2000 LC/MS/MS system. ^{1}H NMR spectra were recorded on a Varian Mercury 400 spectrometer at 400 MHz.

1.2 Synthesis of the ligand LH

The two-step synthesis of the ligand LH is outlined in Scheme 1. The intermediate bis(benzimidazol-2-ylmethyl)amine (a) were prepared according to the literature method [9]. The ligand LH was synthesized using a modified literature procedure[10].

25 mL of sodium hydroxide aqueous solution (0.02 mol·L^{-1}) was added dropwise to a mixture of

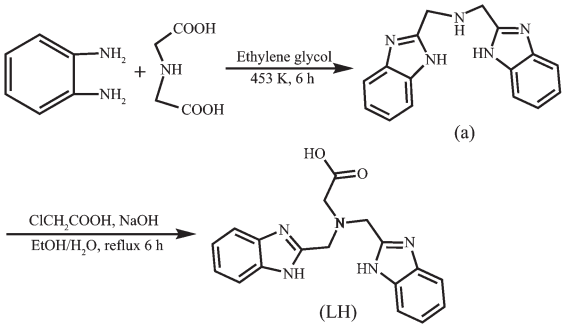

Scheme 1 Synthesis of the ligand LH

chloroacetic acid (0.95 g, 10 mmol) and the intermediate a (2.77 g, 10 mmol) in ethanol (100 mL). The resulting mixture was stirred rapidly and refluxed for 6 hours, then the solvent was evaporated to give the crude product, which was dissolved in water and filtered. The solution was acidified to pH 3~4 with hydrochloric acid (0.1 mol·L^{-1}) and further filtered to obtain the white product. Yield: 2.18 g (65 %). ^{1}H NMR (DMSO-d_6, 400 MHz): 3.42 (s, 2H), 4.28 (s, 4H), 5.06 (s, 2H), 7.25~7.61 (m, 8H), 10.78 (s, 1H). ESI-MS *m/z*: 335.20 (M^+). Anal. Calcd. for $C_{18}H_{17}N_5O_2$ (%): C, 64.47; H, 5.11; N, 21.88. Found (%): C, 64.28; H, 5.41; N, 21.42.

1.3 Synthesis of the cobalt(Ⅱ) complex (1)

The ligand LH (0.34 g, 1 mmol) was dissolved in methanol (40 mL), and the resulting solution was adjusted pH value to 8.0 using 0.5 mol·L^{-1} NaOH. Then $CoCl_2·6H_2O$ (0.24 g, 1 mmol) and $NaClO_4$ (0.12 g, 1 mmol) were added to the stirred solution at 333 K for 6 hours. The solution was cooled to room temperature and filtrated to remove the insoluble substance. Red crystals suitable for X-ray diffraction studies were obtained after five days. m.p. 214~216 ℃. UV-Vis spectra (MeOH solution): 278 nm (ε= 24 400 L·mol^{-1}·cm^{-1}). IR (KBr, cm^{-1}): 3 025 (m), 2 942(s), 1 716(s), 1 545(s), 1 460(s), 1 405(s), 1 056 (m), 755(m). Anal. Calcd. for $C_{72}H_{86}N_{20}O_{23}Co_4Cl_4$(%): C, 43.70; H, 4.35; N, 14.16. Found (%): C, 43.34; H, 4.08; N, 14.42.

1.4 Synthesis of the other complexes (2~7)

The other preparations of transition metal (Mn(Ⅱ), **2**; Fe(Ⅲ), **3**; Ni(Ⅱ), **4**; Cu(Ⅱ), **5**; Zn(Ⅱ), **6**) complexes containing the ligand LH were similar to the cobalt(Ⅱ)

complex (**1**) using metal chlorides (namely, $MnCl_2\cdot 4H_2O$, $FeCl_3\cdot 6H_2O$, $NiCl_2\cdot 6H_2O$, $CuCl_2\cdot 2H_2O$, $ZnCl_2$), but $NaClO_4$ was not added. The dicobalt(Ⅱ) complex $[Co_2(EGTB)(NO_3)_2(DMF)_2](NO_3)_2\cdot 2DMF$ (**7**) was prepared according to the literature[11].

[MnLCl] (**2**): Grey crystalline powder. Yield: 53%, m.p. 282~284 ℃. UV-Vis spectra (MeOH solution): 282 nm (ε=22 840 $L\cdot mol^{-1}\cdot cm^{-1}$). Molar conductance, Λ_M: (DMF, $S\cdot cm^2\cdot mol^{-1}$) 12.5. IR (KBr, cm^{-1}): 3 044 (m), 2 935(s), 1 722(s), 1 578(s), 1 452(s), 1 412(s), 1 066 (m). ESI-MS *m/z*: 424.54 (M^+). Anal. Calcd. for $C_{18}H_{16}N_5O_2MnCl$ (%): C, 50.88; H, 3.77; N, 16.49. Found(%): C, 51.14; H, 3.52; N, 16.02.

[FeLCl]Cl (**3**): Orange crystalline powder. Yield: 42%, m.p.>300 ℃. UV-Vis spectra (MeOH solution): 276 nm (ε=24 510 $L\cdot mol^{-1}\cdot cm^{-1}$). Molar conductance, Λ_M: (DMF, $S\cdot cm^2\cdot mol^{-1}$) 72.8. IR (KBr, cm^{-1}): 3 012 (m), 2 936(s), 1 755(s), 1 568(s), 1 444(s), 1 408(s), 1 036 (m). ESI-MS *m/z*: 425.56 (M^+). Anal. Calcd. for $C_{18}H_{16}N_5O_2FeCl_2$ (%): C, 46.85; H, 3.47; N, 15.18. Found(%): C, 47.08; H, 3.89; N, 14.86.

[NiLCl]$\cdot 2H_2O$ (**4**): Pale-green crystalline powder. Yield: 62%, m.p. 252~253 ℃. UV-Vis spectra (MeOH solution): 272 nm (ε=20 980 $L\cdot mol^{-1}\cdot cm^{-1}$). Molar conductance, Λ_M: (DMF, $S\cdot cm^2\cdot mol^{-1}$) 9.6. IR (KBr, cm^{-1}): 3 048(m), 2 955(s), 1 762(s), 1 526(s), 1 438(s), 1 402(s), 1 048(m). ESI-MS *m/z*: 428.51 $(M-2H_2O)^+$. Anal. Calcd. for $C_{18}H_{20}N_5O_4NiCl$ (%): C, 46.53; H, 4.31; N, 15.08. Found(%): C, 46.16; H, 4.22; N, 15.56.

[CuLCl] (**5**): Green crystalline powder. Yield: 58%, m.p.>300 ℃. UV-Vis spectra (MeOH solution): 276 nm (ε=24 380 $L\cdot mol^{-1}\cdot cm^{-1}$). Molar conductance, Λ_M: (DMF, $S\cdot cm^2\cdot mol^{-1}$) 11.2. IR (KBr, cm^{-1}): 3 052(m), 2 938(s), 1 762(s), 1 555(s), 1 428(s), 1 412(s), 1 026 (m). ESI-MS *m/z*: 433.14 (M^+). Anal. Calcd. for $C_{18}H_{16}N_5O_2CuCl$(%): C, 49.88; H, 3.67; N, 16.17. Found(%): C, 50.14; H, 4.02; N, 16.62.

[ZnLCl] (**6**): Pale-yellow crystalline powder. Yield: 54%, m.p.>300 ℃. UV-Vis spectra (MeOH solution): 278 nm (ε=20 850 $L\cdot mol^{-1}\cdot cm^{-1}$). Molar conductance, Λ_M: (DMF, $S\cdot cm^2\cdot mol^{-1}$) 11.8. IR (KBr, cm^{-1}): 3 048 (m), 2 944(s), 1 732(s), 1 568(s), 1 466(s), 1 422(s), 1 014 (m). ESI-MS *m/z*: 434.55 (M^+). Anal. Calcd. for $C_{18}H_{16}N_5O_2ZnCl$(%): C, 49.71; H, 3.68; N, 16.11. Found (%): C, 49.48; H, 3.26; N, 16.58.

1.5 Structure determination of complex 1

Red crystal of compound **1** having approximate dimensions of 0.30 mm×0.30 mm×0.20 mm was mounted on a glass fiber in a random orientation at 298(2) K. The determination of unit cell and the data collection were performed with Mo $K\alpha$ radiation (λ= 0.071 073 nm) on a Brucker Smart-2000 CCD diffactometer. A total of 16 976 reflections were collected in the range of $1.63°<\theta<25.68°$ at room temperature. The original data were integrated and corrected for Lorentz polarization effects using SAINT program and were corrected for absorption effects[12-13]. Structures were solved by direct methods using SHELXS-97, and all non-hydrogen atoms were directly located from difference Fourier maps and successfully refined with anisotropic displacement parameters[14]. The coordinates of hydrogen atoms only participated in the structure factor calculation and not included in the refinement. Hydrogen atoms in the complexes were placed in idealized positions, and those in water molecules were located in the difference Fourier maps. The Cl(2) and O(5) are both half occupancy. Due to the Cl(2) is too close to O(5), it was necessary to apply SIMU restraints to the O(5) to avoid the high ellipsoid in O(5). Because the guest solvent molecules are highly disordered and impossible to refine using conventional discrete-atom models, the QUEEZE subroutine of the PLATON software suite was applied to remove the scattering from the free water molecules[15]. A SQUEEZE analysis showed that the void space was occupied by 104 electrons per formula, corresponding to 10 water molecules per formula unit. The number of free water molecules were also determined by element analysis. The final R=0.045 9 and wR=0.150 2 ($I>2\sigma(I)$), S= 1.122, $(\Delta/\sigma)_{max}$=0.001, $(\Delta\rho)_{max}$=852 $e\cdot nm^{-3}$ and $(\Delta\rho)_{min}$ =−375 $e\cdot nm^{-3}$. Crystal data and structural refinement were listed in Table 1. The selected bond lengths and bond angles were summarized in Table 2, and the hydrogen bond lengths and bond angles were given in Table 3.

CCDC: 950329, **1**.

Table 1 Crystal data and structure refinements of complex 1

Formula	$C_{72}H_{86}N_{20}O_{23}Cl_4Co_4$	V / nm^3	2.288 0(4)
Formula weight	1 977.13	Z	1
Crystal system	Triclinic	D_c / (g·cm^{-3})	1.435
Space group	$P\bar{1}$	F(000)	1 018
a / nm	1.337 06(12)	Reflections collected, unique	17 071, 8 620
b / nm	1.414 06(13)	R_{int}	0.017 8
c / nm	1.417 54(13)	Data, restrains, parameters	8 620, 18, 548
α / (°)	77.488 0(10)	Final R indices [$I>2\sigma(I)$]	R_1=0.045 9, wR_2=0.150 2
β / (°)	75.624 0(10)	R indices (all data)	R_1=0.051 8, wR_2=0.157 2
γ / (°)	62.574 0(10)	GOF on F^2	1.117

Table 2 Selected bond lengths (nm) and bond angles (°) of complex 1

Cl(1)-Co(1)	0.232 3(7)	O(5)-Co(2)	0.199 1(5)	Cl(2)-Co(2)	0.233 1(2)
Co(1)-O(1)	0.199 1(2)	Co(1)-N(2)	0.203 6(2)	Co(1)-N(4)	0.203 8(2)
Co(1)-N(1)	0.232 2(2)	Co(2)-O(3)	0.199 0(2)	Co(2)-N(9)	0.204 1(2)
Co(2)-N(7)	0.205 2(2)	Co(2)-N(6)	0.227 4(2)	C(9)-N(1)	0.146 7(4)
N(1)-Co(1)-Cl(1)	177.44(6)	O(1)-Co(1)-N(2)	108.98(9)	O(1)-Co(1)-N(1)	77.40(7)
Cl(2)-Co(2)-N(6)	170.11(9)	N(6)-Co(2)-O(5)	171.60(15)	O(3)-Co(2)-N(6)	78.26(8)

Table 3 Hydrogen bond lengths (nm) and bond angles (°)

D–H···A	d(D-H) / nm	d(H···A) / nm	d(D···A) / nm	∠DHA /(°)
N(3)–H(3)···O(4)#3	0.086	0.188	0.270 8(11)	162
N(8)–H(8)···O(8)#1	0.086	0.212	0.278(8)	132
N(10)–H(10)···O(2)#2	0.086	0.196	0.279 1(11)	163
C(5)–H(5)···O(8)#3	0.093	0.245	0.337(7)	171
C(19)–H(19B)···Cl(1)	0.097	0.282	0.378 6(8)	174
C(22)–H(22)···Cl(2)	0.093	0.278	0.344 6(13)	132
C(25)–H(25)···O(8)#1	0.093	0.23	0.296(7)	128
C(27)–H(27A)···O(1)#2	0.097	0.248	0.332 5(9)	145

Symmetry codes: #1: −1+x, y, z; #2: −x, −y, 1−z; #3: 1−x, −y, 1−z.

1.6 Catecholase mimic activity

3,5-di-*tert*-butylcatechol (3,5-DTBC) was used as the substrate to investigate the catalytic activity of the catecholase model complex[7]. Kinetic experiments for the oxidation of 3,5-DTBC were performed spectrophotometrically on a Analytik jena Specord 210 spectrophotometer by the characteristic absorption band of the expected product, 3,5-di-*tert*-butyl-*o*-benzoquinone, at 400 nm. Freshly prepared stock solutions of the complex (0.10 mmol·L^{-1}) and 3,5-DTBC (1.0 mmol·L^{-1}) were used under aerobic conditions at 25 ℃. Oxidative reactions of 3,5-DTBC (0.010 mmol·L^{-1}~1.0 mmol·L^{-1}) were initiated by the addition of the complex (0.010 mmol·L^{-1}) in methanol-tris-HCl (tris=trihydroxymethylaminomethane, 0.01 mol·L^{-1}) buffer solution. The pH values of the reaction system changed in the range of 5~11. The absorbance versus wavelength (wavelength scan) of the solutions was recorded at a regular time interval of 5 min. A kinetic treatment on the basis of the Michaelis-Menten approach was applied and the results were evaluated from Lineweaver-Burk double-reciprocal plots. In each kinetic trial, 8 points were recorded to obtain the kinetic data. The 3,5-DTBC solution in the absence of

the complex was taken as a control.

2 Results and discussion

2.1 Crystal structure of complex 1

In the crystal structure of complex **1** (Fig.1), the asymmetric unit has two cobalt(Ⅱ) ions. One cobalt(Ⅱ) ion is five-coordinated by one chloride ion Cl(1), two benzimidazole nitrogen atoms (N(2), N(4)), one carboxy oxygen atom O(1) and one amine nitrogen atom (N(1)) of the ligand LH, forming a distorted trigonal biyramid coordination geometry (angular structural parameter (τ) equals to 0.96)[16]. Cl(1) and N(1) occupy the axial position, and N(2), N(4) and O(1) located in the equatorial plane. The Cl(1)-Co(1)-N(1) bond angle is 177.35(6)°, which is slightly deviated from ideal 180° (Table 1). However, the other cobalt(Ⅱ) ion is partly coordinated by one water oxygen atom (O(5)) (or one chloride ion Cl(2)), which is unusual for such complex. Similar example has also been reported for $[Cu(4\text{-atrz})_4(Cl)_{0.5}(H_2O)_{0.5}](ClO_4)_{1.5}$ with equal Cl/O ratio in the same position, and this may offer an opportunity to fine control over the Cl/O composition and properties for the complex[17]. Since the Cl(2) is half occupancy, the ClO_4^- ion is located to balance the charge. N(6) and O(5) (or Cl(2)) reside in the axial position, and N(7), N(9) and O(3) make up the equatorial plane. The Co-N bond distances range from 2.035(2) to 2.320(2) nm, and the distance of Co-N(amino) is obviously longer than that of Co-N(benzimidazole), thus forming a distorted trigonal biyramid coordination geometry (τ=0.80). It′s also found that the carboxyl group is deprotonized, which leads to a single negative charge ligand L^-. The dihedral angles between two benzimidazole rings of the deprotonized ligand L^- in the unit cell are 56.68° and 56.01°, respectively. As shown in Table 2 and Fig.2, the uncoordinated anion ClO_4^- and water molecules participate in the formation of hydrogen bonds. The molecules are stabilized by intermolecular N–H⋯O, C–H⋯O and C–H⋯Cl hydrogen bonds, leading to the formation of a three dimension network.

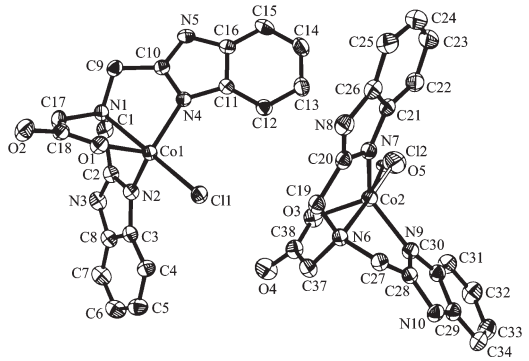

Ellipsoids are at the probability level of 30%, and the noncoordinating; ClO_4^- and solvent water molecules are omitted for clarity

Fig.1　An ORTEP view of Structure of complex **1**

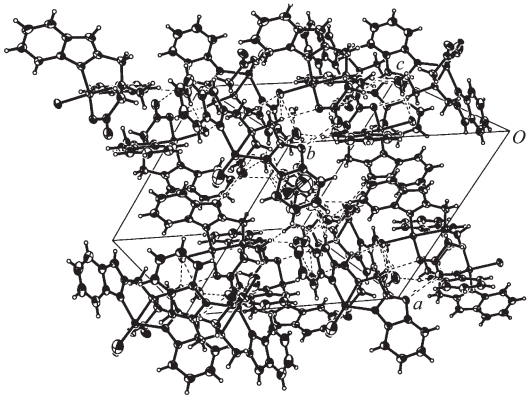

Fig.2　Packing of complex **1** in unit cell

2.2 Studies of catecholase activity

3,5-DTBC has been widely chosen as a substrate in catecholase model complex studies. It′s readily oxidized to the corresponding 3,5-di-*tert*-butyl-o-quinone (3,5-DTBQ) owing to its low redox potential, and its bulky substituents prevent further reactions such as ring opening[18]. 3,5-DTBQ is considerably stable and has a strong absorption at λ_{max}=400 nm (ε= 1 900 $L\cdot mol^{-1}\cdot cm^{-1}$), so that the activity and reaction rate could be determined using UV spectroscopy[19]. Fig.3 showed the variation of the spectral behavior of complex **1** (0.01 $mmol\cdot L^{-1}$) in the presence of 3,5-DTBC (100 equiv.) under aerobic conditions. The band that corresponded to 3,5-DTBQ was observed at 400 nm after addition of the substrate (3,5-DTBC) to the solution of complex **1**.

The kinetic studies on the oxidation of 3,5-DTBC were carried out by the method of initial rates. It′s found that the reaction between complex **1** and substrate (3,5-DTBC) was a first order reaction, so

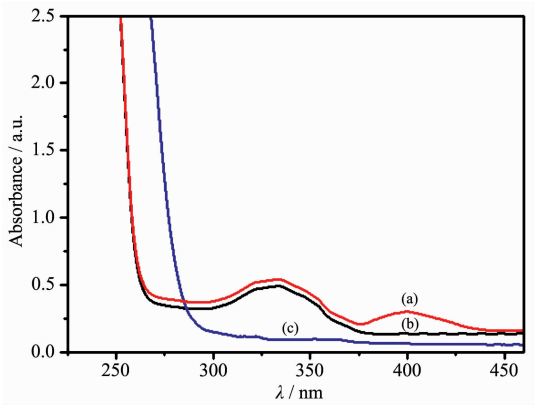

Fig.3 UV-Vis spectra of the methanol solution of complex **1** (0.1 mmol·L^{-1}) after addition of 3,5-DTBC (10 mmol·L^{-1}) for 4 h (a), complex **1** (b) and 3,5-DTBC (c)

their relationship could be described using a formula: $\ln[(A_f-A_i)/(A_f-A_t)]=kt$[20]. Here, k is the rate constant, A_f, A_i and A_t were the final, initial and the time t absorbance of the reaction solution, respectively. The maximum absorbance of the growth of the quinone (3,5-DTBQ) at 400 nm was measured as a function of time, and Fig.4 showed a linear relationship in the $\ln[(A_f-A_i)/(A_f-A_t)]$ versus reaction time (t) plot in the presence of complex **1**. The effect of the complexes (**1**~**7**) concentration on the oxidation of 3,5-DTBQ was also observed at pH 9.0 and 25 ℃ (Fig.5). The reaction rate was initially increased linearly with increasing concentration of these complexes, indicating a first-order dependence on each complex concentration. As shown in Fig.6, the pH dependence of the catecholase activity was promoted by the complexes (**1**~**7**) in the

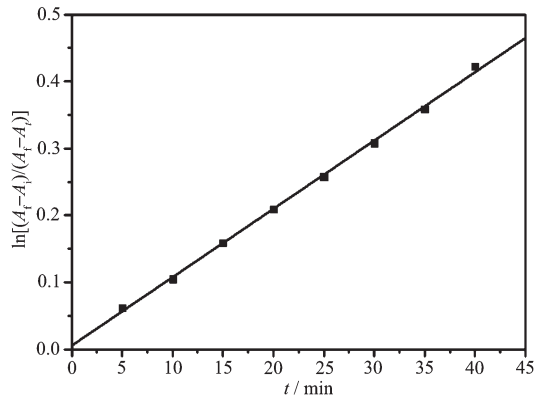

$c_{complex\ 1}$=5.0×10^{-5} mol·L^{-1}, $c_{3,5\text{-DTBC}}$=1.0×10^{-3} mol·L^{-1}

Fig.4 Plot of $\ln[(A_f-A_i)/(A_f-A_t)]$ versus the reaction time at pH 9.0 and 25 ℃

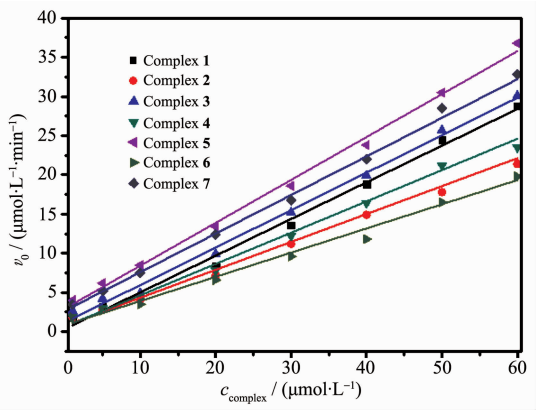

Fig.5 Complexes (**1**~**7**) dependence of oxidation of 3,5-DTBC (1 mmol·L^{-1}) at pH 9.0 and 25 ℃

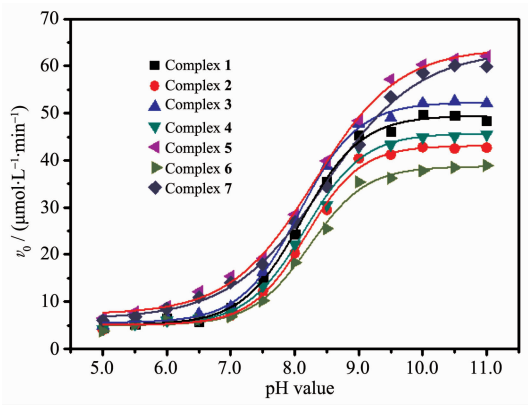

Fig.6 pH value dependence for the oxidation of 3,5-DTBC catalyzed by the complexes (**1**~**7**)

range of 5.0~11.0. The plots of v_0 (initial rate) vs pH value were observed to exhibit sigmoid-shape profiles, and the catalytic activities of all complexes were nearly increased in the pH value range from 7.0 to 9.0.

The data depicted in Fig.7 revealed saturation kinetics of complex **1** with Michaelis-Menten-like

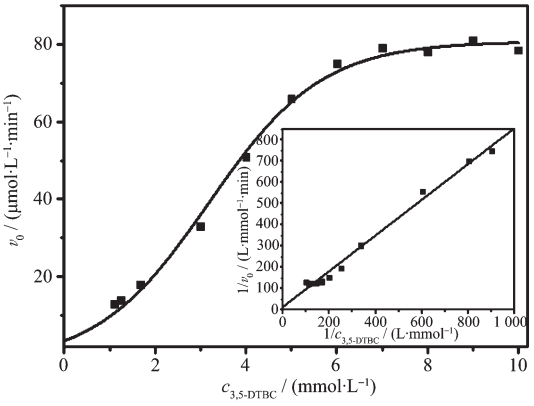

Inset: Lineweaver-Burk double reciprocal plot

Fig.7 Plot of the reaction rates vs concentration of 3,5-DTBC for complex **1**

behavior. So an analysis based on the Michaelis-Menten model, originally developed for enzyme kinetics, was applied. The Michaelis-Menten equation is usually expressed as following:

$$v=\frac{v_{max}c_s}{K_m+c_s},\ v_{max}=k_{cat}c_M \quad (1)$$

Here, v_{max} is the maximum initial rate, K_m is Michaelis constant, k_{cat} is the turnover number, namely, the amounts (mol) of substrate converted to product per minute per mole of mimetic enzyme. c_S and c_M are the concentrations of substrate and model complex, respectively. The Michaelis-Menten equation can be turned into Lineweaver-Burk equation by taking its double reciprocal:

$$\frac{1}{v}=\frac{K_m}{v_{max}}\cdot\frac{1}{c_s}+\frac{1}{v_{max}} \quad (2)$$

The inset in Fig.7 showed $1/v_0$ was linear with $1/c_{3,5\text{-DTBC}}$ for complex **1**, implying a first order reaction dependence. The slope of the straight line was K_m/v_{max}, and the intercept on the vertical axis was $1/v_{max}$. Several kinetic parameters v_{max}, K_m and k_{cat} were calculated from the Lineweaver-Burk plot model (Table 4). It is found that k_{cat} of complex **1** toward 3,5-DTBC increased from 4.35 min^{-1} (20 ℃) to 13.55 min^{-1} (45 ℃). So the catalytic activity of complex **1** increased with increasing of temperatures. The kinetic data of the complexes (**1**~**7**) were also measured at pH 9.0 and 25 ℃. As shown in Table 5, the catalytic activity of these complexes were easily arranged in descending order: **3** > **7** > **5** > **1** > **4** > **2** > **6**. The catecholase model complexes have been reported to relate to several factors such as metal-metal distance, lability of exogenous ligands, coordination configuration and electrochemical properties[21]. Of all the complex, **3** showed the best catalytic activity, its difference with the other complexes (**1**, **2**, **4**, **5**, **6**) could be attributed to the redox potential effect of various metal ions on the catecholase model complexes, and the results were in accordance with the literatures reported previously[11,22-23]. The catalytic activity of complex **7** was better than complex **1**, because the former was a dicobalt (Ⅱ) complex, which may be dependent upon the interaction between each active center and substrate due to its long dinuclear distance[11]. A probable explanation for the catecholase catalytic reactivity of complex **1** was mainly related to its coordination environment. The five-coordinated cobalt(Ⅱ) ion has an unsaturated vacancy, and it could combine with the substrates[7,11].

Table 4　Kinetic data of complex 1 at pH 9.0

T / ℃	v_{max} / (mmol·L^{-1}·min^{-1})	K_m / (mmol·L^{-1})	k_{cat} / min^{-1}
20	1.98×10^{-2}	2.06	4.35
25	3.12×10^{-2}	4.55	6.56
30	4.88×10^{-2}	5.58	8.69
35	5.84×10^{-2}	7.02	9.52
40	7.12×10^{-2}	8.96	10.78
45	9.06×10^{-2}	10.24	13.55

Table 5　Kinetic data of the complexes 1~7 at pH 9.0 and 25 ℃

Complex	v_{max} / (mmol·L^{-1}·min^{-1})	K_m / (mmol·L^{-1})	k_{cat} / min^{-1}
1	3.12×10^{-2}	4.55	6.56
2	2.56×10^{-2}	3.64	5.05
3	4.92×10^{-2}	5.86	8.14
4	2.96×10^{-2}	3.82	6.21
5	3.18×10^{-2}	4.74	6.88
6	2.18×10^{-2}	3.32	5.01
7	3.98×10^{-2}	5.38	7.12

3 Conclusions

In summary, we have prepared a cobalt(Ⅱ) complex, which was characterized by single crystal X-ray diffraction. The complex showed pH value dependence for the oxidation of 3,5-DTBC in the range of 5 ~11, and the kinetics of 3,5-DTBC catalyzed by the complex obeyed the Michaelis-Mentent equation, its catecholase catalytic activity increased with the rise of the temperature.

References:

[1] Koval I A, Gamez P, Belle C, et al. *Chem. Soc. Rev.*, **2006**, **35**:814-840

[2] Klabunde T, Eicken C, Sacchettini J C, et al. *Nat. Struct. Biol.*, **1998**,**5**:1084-1090

[3] Patra A, Giri G C, Sen T K, et al. *Polyhedron*, **2014**,**67**:495-504

[4] Caglar S, Aydemir I E, Adiguzel E, et al. *Inorg. Chim. Acta*, **2013**,**408**:131-138

[5] Caglar S, Adiguzel E, Caglar B, et al. *Inorg. Chim. Acta*, **2013**, **397**:101-109

[6] Safaei E, Sheykhi H, Wojtczak A, et al. *Polyhedron*, **2011**, **30**:1219-1224

[7] ZHANG Yong(张勇), ZHOU Xia(周霞), HU Jia-Wei(胡家尾), et al. *Chinese J. Struct. Chem.*(结构化学), **2013**,**32**(9): 1291-1296

[8] Apurba B, Lakshmi K D, Michael G B D, et al. *Inorg. Chem.*, **2012**,**51**:7993-8001

[9] CHEN Yan-Guo(陈彦国), LIAO Zhan-Ru(廖展如), LI Wu-Ke(李武客), et al. *Acta Chim. Sinica*(化学学报), **2000**,**58** (10):1191-1195

[10]Ogawa K, Nakata K, Ichikawa K. *Chem. Lett.*, **1998**,**27**:797-798

[11]Zhang Y, Meng X G, Liao Z R, et al. *J. Coord. Chem.*, **2009**,**62**:876-885

[12]*SAINT, Program for Area Detector Absorption Correction*, Siemens Analytical X-Ray Instruments Inc., Madison, WI 53719, USA, **1994-1996**.

[13]Sheldrick G M. *SADABS, Program for Siemens Area Detector Absorption Correction*, University of Göttingen, Germany, **1996**.

[14]Sheldrick G M. *SHELXS*-97, *Program for the Solution of Crystal Structures*, University of Göttingen, Germany, **1997**.

[15]Spek A L. *Acta Crystallogr.*, **2009**,**D65**:148-155

[16]Addison A W, Rao T N, Reedijk J, et al. *J. Chem. Soc. Dalton Trans.*, **1984**:1349-1356

[17]Yi L, Du J Y, Liu S, et al. *J. Chem. Res.*, **2004**,**1**:29-31

[18]Rompel A, Fischer H, Meiwes D, et al. *FEBS Lett.*, **1999**, **445**:103-110

[19]Seneque O, Campion M, Douziech B, et al. *Eur. J. Inorg. Chem.*, **2002**,**8**:2007-2014

[20]Chen Z F, Liao Z R, Li D F, et al. *J. Inorg. Biochem.*, **2004**, **98**:1315-1318

[21]Neves A, Rossi L M, Bortoluzzi A J, et al. *J. Braz. Chem. Soc.*, **2001**,**12**:747-754

[22]Qiu J H, Liao Z R, Meng X G. *Polyhedron*, **2005**,**24**:1617-1623

[23]Lu L J, Song Y Y, Liu H, et al. *J. Coord. Chem.*, **2012**,**65**: 1278-1288